

Supporting Information for

Pillar-layered Ni₂P-Ni₅P₄-CoP array derived from metal-organic framework as a bifunctional catalyst for efficient overall water splitting

Qihang Nie, Zixian Zhu, Yan Wang, Chengyu Jiang, Min Wang* and Xiang Zhang*

1. Experimental Procedures

1.1 Chemicals and reagents: Cobalt nitrate hexahydrate, 1,4-dicarboxybenzene, polyvinyl pyrrolidone (Mw = 58000), NaH₂PO₂, KOH, 20% Pt/C and RuO₂ were purchased from Sigma Aldrich. DMF, EtOH and acetone were also purchased from Sigma Aldrich. These chemicals and reagents above were analytically pure and used as received without further purification. The ultra-pure water was obtained through a Millipore system. Nickel foam (NF) (thickness: 1.7 mm, purchased from Sigma Aldrich) was wash with 3M HCl, water and acetone in turn and dried in a vacuum oven at 60 °C before use.

1.2 Preparation Procedures

Preparation of Ni-MOF/NF and Ni-Co-MOF /NF

NF was used as support and nickel source to grow Ni-Co pillar-layered structure by a solvothermal reaction. Typically, 1,4-dicarboxybenzene (H₂BDC, 38.0 mg) and polyvinyl pyrrolidone (125.0 mg) were dissolved in 20.0 mL solution (DMF: EtOH = 1:1) as solution A. A certain amount of cobalt nitrate hexahydrate (250.0 mg) was dissolved in 10.0 mL water as solution B. The solution A and solution B was mixed and sonicated for 20 minutes. And then the mixture was transferred to an autoclave. The fresh NF (2.0 cm * 3.0 cm) was immersed into the autoclave and the autoclave was heated at 95 °C for 6 hours subsequently. After the reactant was cooled to room temperature, the Ni-Co pillar-layered structure growing *in-situ* on the NF was well prepared (donated as Ni-Co-MOF/ NF). After washed by EtOH and H₂O, the Ni-Co-MOF/NF was dried for further synthesis. For comparison, Ni-MOF/NF, was prepared through a similar procedure without the addition of Co salt.

Preparation of Ni₂P-Ni₅P₄-CoP-C/NF, Ni₂P-Ni₅P₄-C/NF and Ni₂P -CoP-C/NF.

Sodium hypophosphite was selected as P source for the preparation of heterogenous TMPs in this work, which release PH₃ during heating. As precursor, Ni-Co-MOF/NF was put in the middle of tube furnace and sodium hypophosphite (1.0 g) in another porcelain boat was put upstream. Subsequently, the samples were

treated to 350 °C and hold for 1.5 hours. Pure argon was selected as the carrier gas and the gas flow rate was 75.0 mL/min. After phosphorization, a pillar-layered Ni₂P-Ni₅P₄-CoP-C array assembled on the conductive NF was obtained with loading amount around 3.5 mg cm⁻². The Ni₂P-Ni₅P₄-C/NF was prepared through the same treatment from Ni-MOF/NF and the loading is 2.9 mg cm⁻². In addition, the Ni₂P-CoP-C/NF was prepared through the similar process except for that the phosphorization temperature is 300 °C and the loading amount is also around 3.5 mg cm⁻².

1.3 Materials characterization

The scanning electron microscopy images of the self-supporting MOFs and TMPs were performed on the JEOL scanning electron microscope (JSM-7900F) equipped with an energy dispersive X-ray spectrometry. While, Transmission electron microscopy images of samples were investigated on a JEM-2100F JEOL electron microscopy under the electron acceleration energy of 200 kV. The measurement of actual crystal phase the self-supporting Ni/Co based structure was collected on a Rigaku Smart Lab X-ray rotation diffractometer equipped with a Cu K α radiation ($\lambda = 1.5418 \text{ \AA}$). The X-ray photoelectron investigation of heterogenous TMP was carried on a Thermo Fisher Esca Lab 250Xi equipped with a monochromatic Al K α source as the excitation source ($E_{\text{photon}} = 1486.6 \text{ eV}$)

1.4 Electrochemical measurements

Electrocatalytic performance of the heterogenous TMPs and contrast were tested on a CHI 760D electrochemical analyzer (CH Instruments, Inc., Shanghai). The 20% Pt-C or RuO₂ was dropped on the NF with loading of 3.5 mg cm⁻² for the electrochemical test. A classic three-electrode system was applied, wherein the carbon rod and mercury oxide electrode (in 1.0 M KOH solution) was used as the counter electrode and the reference electrode, respectively. All tests were conducted at room temperature.

The HER performance of all samples was tested in N₂-saturated 1.0 M KOH solutions. While, the OER performances were evaluated in O₂-saturated 1.0 M KOH solution. The linear sweep voltammetry (LSV) curve for HER and OER was obtained with a scan rate of 5 mV/s and 1 mV/s, respectively. Nyquist plots of Ni-Co based heterostructures were obtained in the frequency range of $1 \times 10^{-2} \sim 10^6 \text{ Hz}$ at -0.1 V. In HER, the catalytic stability assessment of the Ni₂P-Ni₅P₄-CoP-C/NF through cyclic voltammetry was performed between 0 and -0.22 V at a sweep rate of 0.1 V/s. While

in OER, the test was performed between 1.21 and 1.61 V.

In the investigation of HER and OER, the applied voltage versus (*vs.*) reversible hydrogen electrode (RHE) were presented with 90% *iR* correction manually as Eqs.

(1):

$$E_{\text{RHE}} = E_{\text{Hg/HgO}} + 0.05916 \text{ pH} + 0.098 \text{ V} - 0.90 iR_s, R_s = 2.1 \Omega. \quad (1)$$

CV measurements to evaluate C_{dl} were performed at the scan rate of 0.02, 0.04, 0.06, 0.08 and 0.1 V s^{-1} in the non-Faradaic range. The calculation of C_{dl} follows Eqs. (2):

$$C_{\text{dl}} = (j_a - j_c) / (2 * \nu) = (j_a + |j_c|) / (2 * \nu) = \Delta j / (2 * \nu) \quad (2)$$

Wherein j_a and j_c represent the anodic and cathodic current density recorded at the middle of the selected potential range and ν represents the scan rate.

The overall water splitting investigation was carried out on the $\text{Ni}_2\text{P-Ni}_5\text{P}_4\text{-CoP-C/NF} \parallel \text{Ni}_2\text{P-Ni}_5\text{P}_4\text{-CoP-C/NF}$ couple in a two-electrode system in 1.0 M KOH solution. The scan rate of linear sweep voltammetry in overall water splitting was 1 mV/s. The applied voltage *vs.* RHE of the overall water splitting measurement were presented without *iR* correction.

Figures and tables

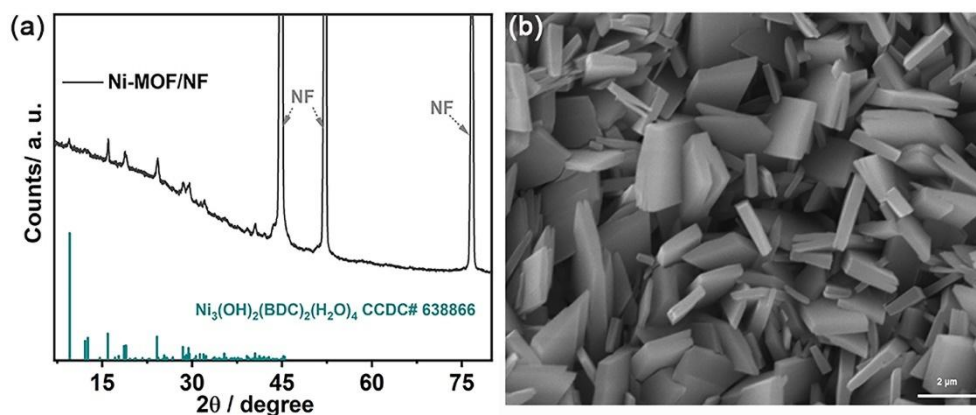


Figure S1 (a) XRD pattern and (b) SEM image of Ni-MOF/NF.

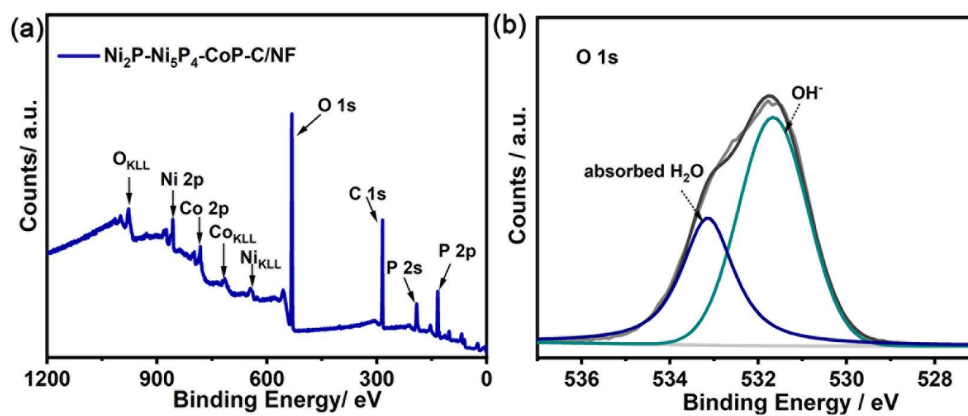


Figure S2 (a) XPS survey spectrum and (b) $\text{O } 1s$ spectrum of $\text{Ni}_2\text{P-Ni}_5\text{P}_4\text{-CoP-C/NF}$.

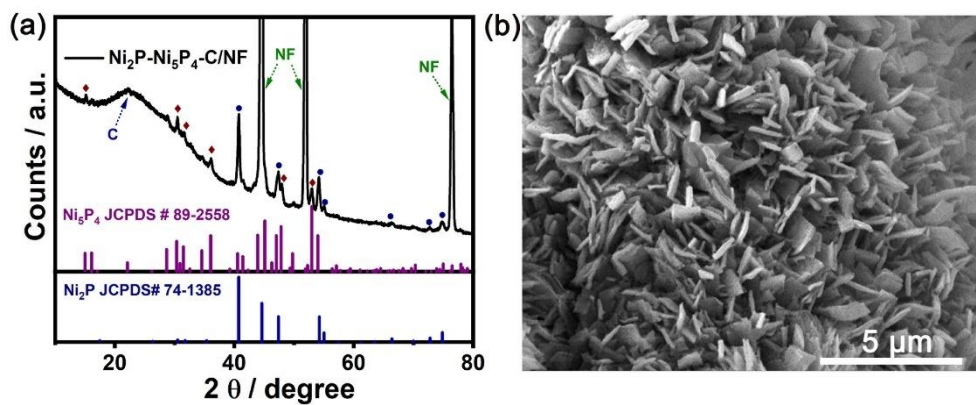


Figure S3 XRD pattern (a) and SEM image (b) of $\text{Ni}_2\text{P-Ni}_5\text{P}_4\text{-C/NF}$.

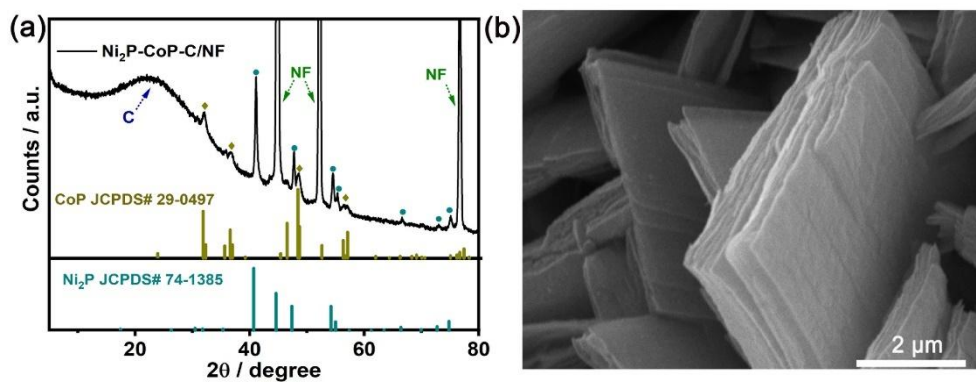


Figure S4 XRD pattern (a) and SEM image (b) of Ni₂P-CoP-C /NF.

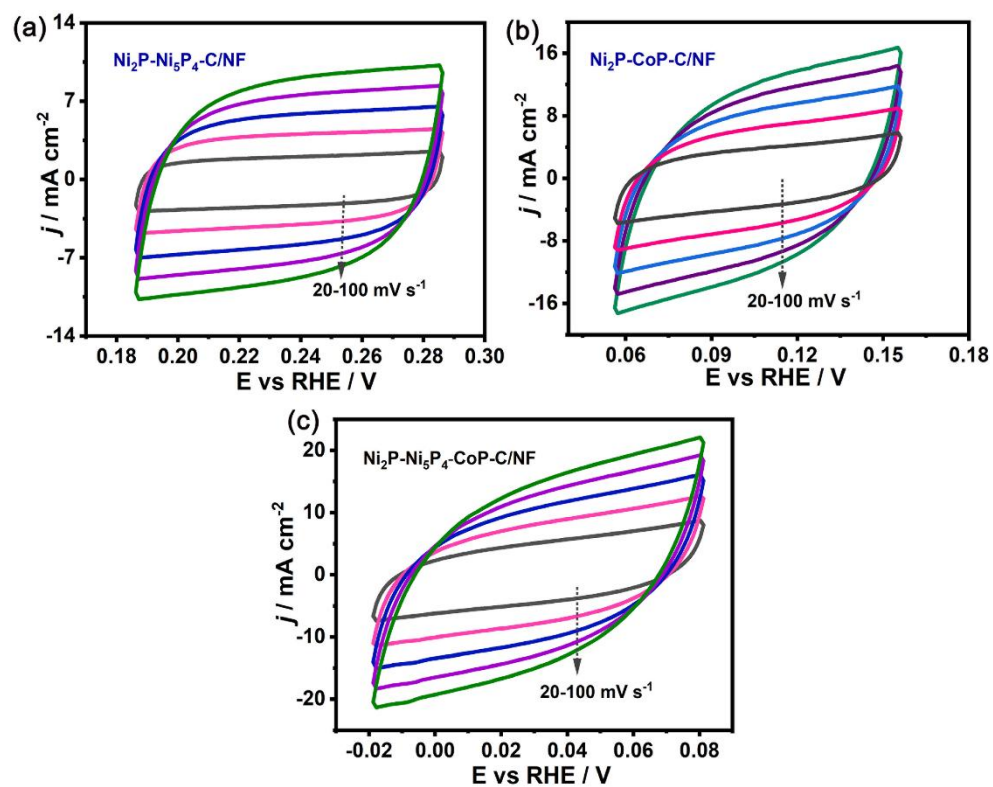


Figure S5 Cyclic voltammetry curves of (a) $\text{Ni}_2\text{P-Ni}_5\text{P}_4\text{-C/NF}$, (b) $\text{Ni}_2\text{P-CoP-C/NF}$ and (c) $\text{Ni}_2\text{P-Ni}_5\text{P}_4\text{-CoP-C/NF}$ at the scan rate of 20, 40, 60, 80, 100 mV s^{-1} respectively in 1.0 M KOH solution in the non-Faradaic region.

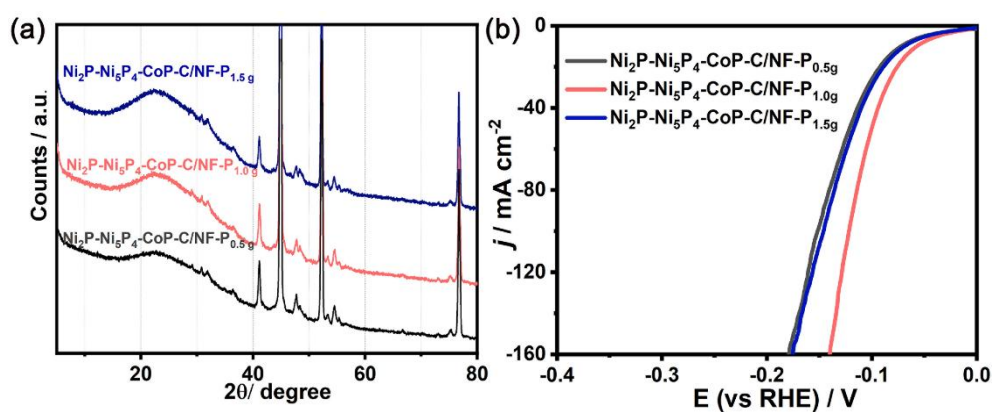


Figure S6 (a) XRD pattern and (b) LSV curve of $\text{Ni}_2\text{P-Ni}_5\text{P}_4\text{-CoP-C/NF}$ towards HER in 1.0 M KOH solution at a scan rate of 5 mV s^{-1} , which was prepared by varying the amount of NaH_2PO_2 at 0.5 g, 1.0 g and 1.5 g at $350 \text{ }^\circ\text{C}$ respectively.

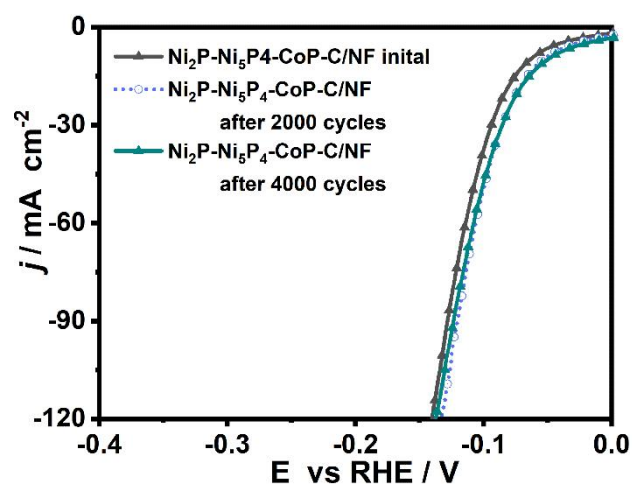


Figure S7 Polarization curve the Ni₂P-Ni₅P₄-CoP-C/NF towards HER before and after 2000 and 4000 cycles.

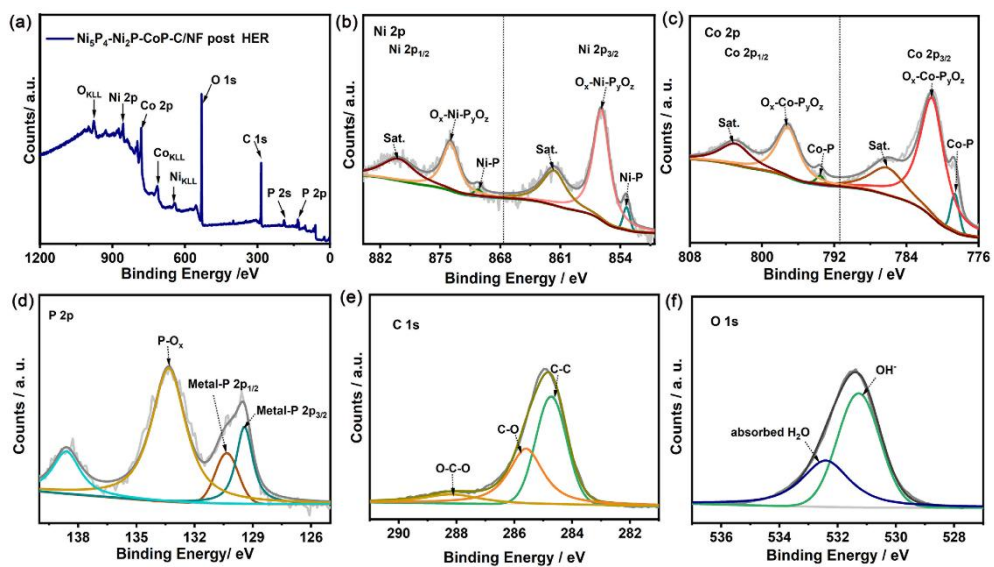


Figure S8 XPS spectra of (a) survey-scan spectrum, (b) Ni 2p, (c) Co 2p, (d) P 2p, (e) C 1s and (f) O 1s performed on $\text{Ni}_5\text{P}_4\text{-Ni}_2\text{P-CoP-C/NF}$ after continuous electrolysis towards HER

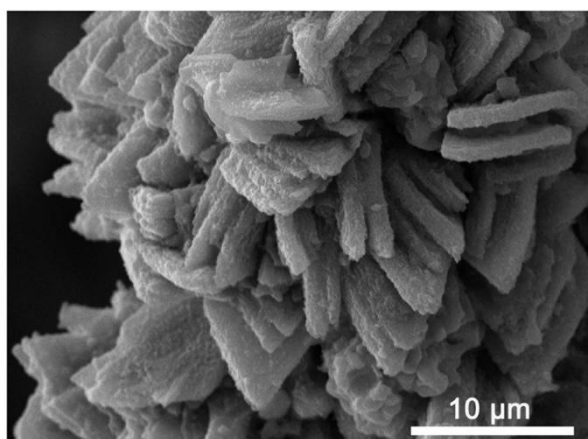


Figure S9 SEM image of $\text{Ni}_5\text{P}_4\text{-Ni}_2\text{P-CoP-C/NF}$ after continuous electrolysis towards HER.

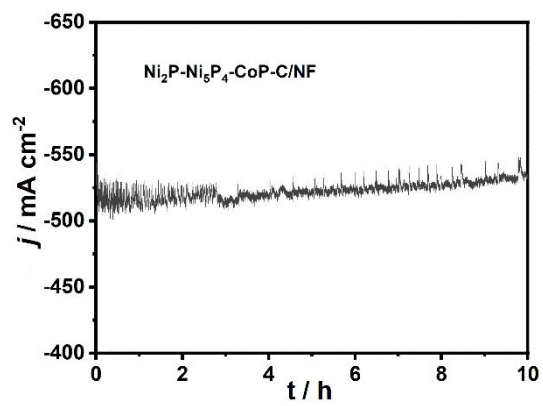


Figure S10 Chronoamperometry of Ni₂P-Ni₅P₄-CoP-C/NF towards HER in 1.0 M KOH aqueous under -315mV.

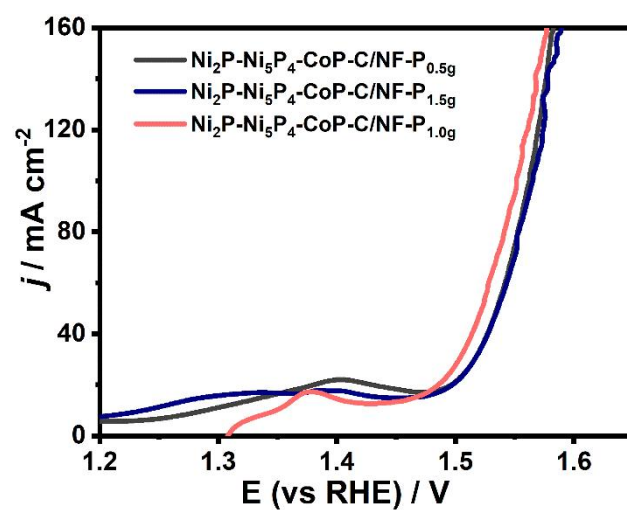


Figure S11 Polarization curves of Ni₂P-Ni₅P₄-CoP-C/NF towards OER in 1.0 M KOH solution at a scan rate of 1 mV s⁻¹, which was prepared by varying the amount of NaH₂PO₂ at 0.5 g ,1.0 g and 1.5 g respectively.

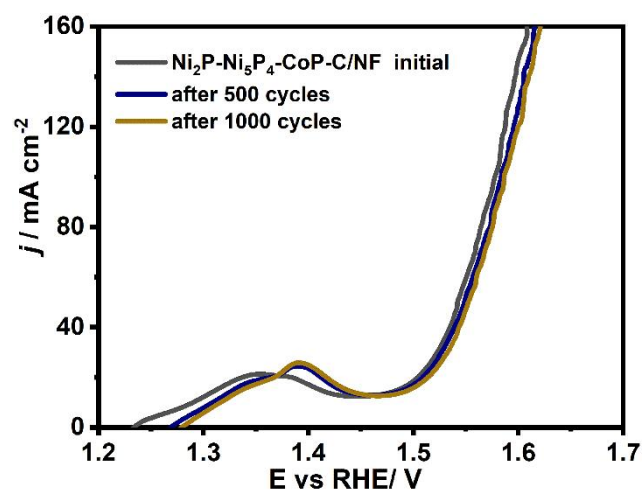


Figure S12 Polarization curve the $\text{Ni}_2\text{P-Ni}_5\text{P}_4\text{-CoP-C/NF}$ towards OER before and after 1000 cycles.

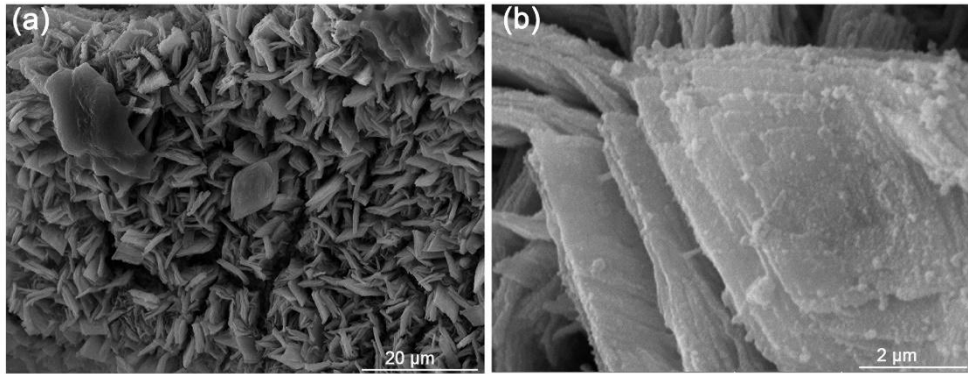


Figure S13 SEM images of $\text{Ni}_5\text{P}_4\text{-Ni}_2\text{P-CoP-C/NF}$ after 1000 CV cycles towards OER in 1.0 M KOH.

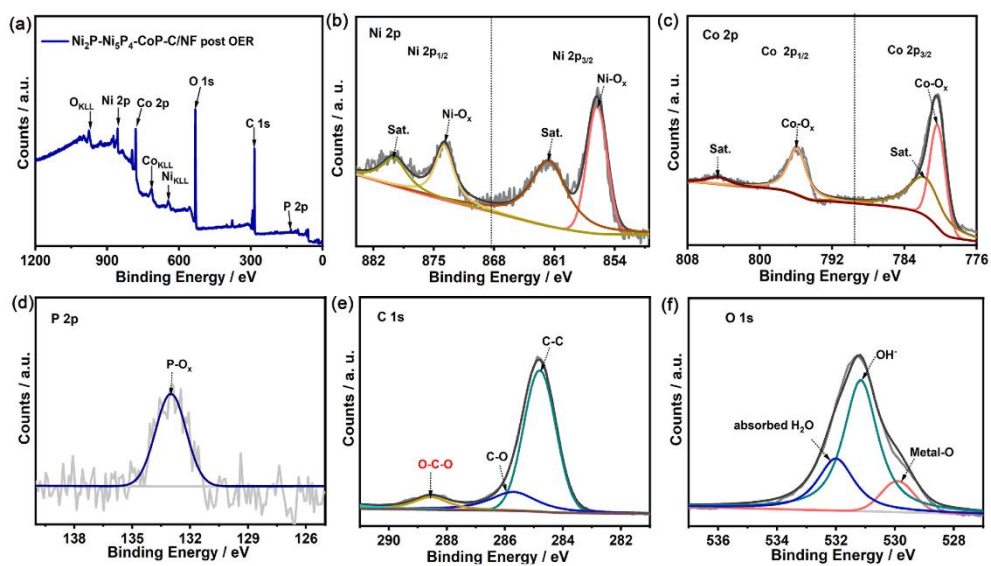


Figure S14 XPS spectra of (a) survey-scan spectrum, (b) Ni 2p, (c) Co 2p, (d) P 2p, (e) C 1s and (f) O 1s performed on $\text{Ni}_5\text{P}_4\text{-Ni}_2\text{P-CoP-C/NF}$ after 1000 CV cycles towards OER.

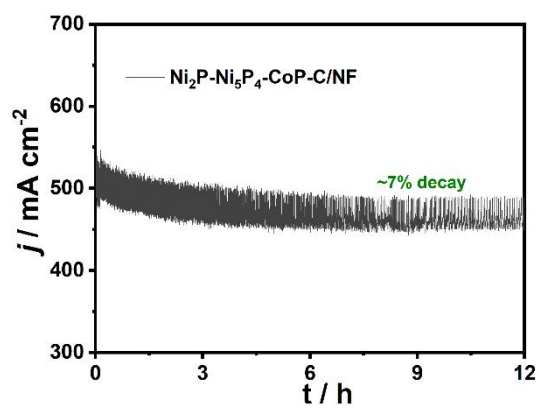


Figure S15 The current density-time (j - t) curve toward sOER on $\text{Ni}_2\text{P-Ni}_5\text{P}_4\text{-CoP-C/NF}$ in 1.0 M KOH aqueous under 1.79 V.

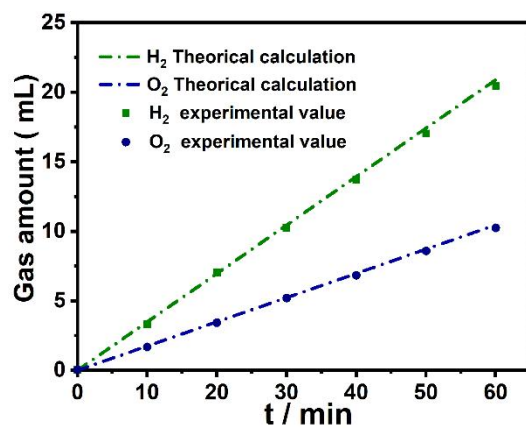


Figure S16 The theoretically calculated and experimentally measured amount of H₂ and O₂ of Ni₂P-Ni₅P₄-CoP-C/NF towards overall water splitting at 50 mA versus time.

Table S1 Comparison of HER, OER and overall water splitting performance of heterogenous TMPs with some previous report in 1.0 M KOH solution.

Catalyst	HER (η_{10} /mV)	OER (η_{10} /mV)	OWS (η_{10} /V)	Reference
Ni ₂ P- Ni ₅ P ₄ -CoP-C/NF	-58	293 (η_{50})	1.55	This work
Ni ₂ P-NiP ₂ HNP _s /NF	-59.7	--	--	<i>Adv. Mater.</i> , 2018, 30 , 1803590.
CoP/NiCoP/NC	-75	--	--	<i>Adv. Funct. Mater.</i> , 2019, 29 , 1807976.
Co-Fe-P	-86	--	--	<i>Nano Energy</i> , 2019, 56 , 225.
C(N,P),Co ₃ P -FeP/ CC	-50(η_2)	--	--	<i>J. Electroanal. Chem.</i> ,2021, 895 , 115521.
CoP@CoP@(Co/Ni) ₂ P	-147	--	--	<i>Chem. Eng. J.</i> , 2023, 463 ,142448.
Ni ₂ P-CoP	-105 (0.5 M H ₂ SO ₄)	320	--	<i>ACS Appl. Mater. Interfaces</i> , 2017, 9 , 23222.
Cu ₃ P· _{0.75} Co ₂ P	-124.6(η_{20})	334	1.55	<i>Nanoscale</i> , 2019, 11 , 6394.
CoP-FeP/CC	-71	250	--	<i>ACS Sustainable Chem. Eng.</i> , 2019, 7 , 2335.
Ni ₂ P-Ni ₃ P ₄ /CC	-102	--	1.69	<i>J. Colloid Inter. Sci.</i> , 2019, 552 , 332.
Co _{0.17} Fe _{0.79} P/NC	-139	299	1.66	<i>ACS Appl. Energy Mater.</i> , 2019, 2 , 2734.
Ni ₂ P-Co ₂ P@C/NF	-167(η_{50})	290(η_{50})	--	<i>Electrochim. Acta</i> , 2019, 318 , 244.
Cu ₃ P-Co ₂ P/NF	-124.6(η_{20})	334(η_{20})	1.55	<i>Nanoscale</i> , 2019, 11 , 6394.
CoP/MoP@NC/CC	94	270	1.71(η_{50})	<i>Appl. Catal. B-Environ.</i> , 2019, 245 , 528.
CC-NC-NiFeP	-94	145	1.54	<i>Nanoscale</i> , 2020, 12 , 8443.
Ni ₁ Co ₁ P	-169	330	--	<i>J. Alloys Compd.</i> , 2020, 847 , 156514.
CoP@FeCoP/NC	-141	238	1.68	<i>Chem. Eng. J.</i> , 2021, 403 , 126312.
MoS ₂ /C (CoP •CNT)	-195	234	--	<i>Chem. Eng. J.</i> , 2021, 419 , 129977.
NiFeP@NiP@NF	-105	227	1.57	<i>ACS Appl. Mater. Interfaces</i> , 2021, 13 , 23702.
Co ₂ P/CoP-NC	-91	292	1.61	<i>Sustain. Mater. Techno.</i> , 2022, 32 ,00421.
CoP-NC@NiFeP	-162	270	1.57	<i>Chem. Eng. J.</i> , 2022, 428 , 131115.
Ni-Fe-Mn-P/NC@NF	-72	274(η_{30})	1.52	<i>J. Mater. Chem. A</i> , 2022, 10 , 16457.
NiFeP/NF	-350(η_{50})	204(η_{50})	1.81(η_{50})	<i>New J. Chem.</i> , 2023, 47 , 737.
Fe-Ni ₂ P/Ni ₅ P ₄ @NC/N F	-105	280 (η_{50})	1.56	<i>Inorg. Chem.</i> , 2023, 62 , 6518.
CoP@Ni/Fe-P	-125	250	1.56	<i>Dalton Trans.</i> , 2023, 52 , 11941.
Ni ₂ P-MoP@NC	-69	249	1.54	<i>J. Mater. Chem. A</i> , 2023, 11 , 15033.
C@CoP-FeP/FF	-154 (η_{50})	297 (η_{100})	1.74 (η_{100})	<i>Small</i> , 2023, 19 , 2206533.
Ni ₃ N-VN/NF	-64	306(η_{50})	1.51	<i>Adv. Mater.</i> , 2019, 1901174.
Ni ₂ P-VP ₂ /NF				
Ni-CoP/Co ₂ P@NC	-117	272	1.59	<i>Chem. Eng. J.</i> , 2022, 433 , 133523.
Hy-Ni-CoP/Co ₂ P@NC				
CoP/CoFeP	---	266	--	<i>ACS Nano</i> , 2023, 17 , 22744.
CoP-Ni ₂ P/NF	--	255	--	<i>Fuel</i> , 2023, 348 , 128509.
Ni ₂ P-CoP/NC	--	267	--	<i>Int. J. Hydrogen Energy</i> , 2024, 54 , 1487.